GALVANOMAGNETIC ROTATION CHARACTERISTICS OF THIN PERMALLOY FILMS AT UNIAXIAL STRESS

By H. RATAJCZAK

Institute of Molecular Physics, Polish Academy of Sciences, Poznań*

(Received November 29, 1977)

The influence of uniaxial mechanical stress on the behaviour of galvanomagnetic voltage in a thin permalloy films, placed in a magnetic field which direction rotates in the sample plane has been studied. On the simple coherent rotation model, a general equation is derived for the galvanomagnetic voltage vs the applied magnetic field and its direction as well as the mechanical stress and its direction. Some particular direction of stress are considered, for which rotation curves are plotted. The curves are compared with the experimental results and show a relatively good agreement in shape of the curves in most cases. However, certain discrepances occure due to angular dispersion of anisotropy.

1. Introduction

Investigations of the elastomagnetic effect on the magnetization reversal process in thin ferromagnetic films have been reported in numerous papers (e.g. [1–6]). Galvanomagnetic effect was found to provide a convenient method for those studies [7, 8]. In the paper [9] elastogalvanomagnetic effect has been considered on the basis of Stoner-Wohlfarth model. However, for same cases, especially when the external magnetic field is absent or applied perpendicularly to the easy axis, this model is unfulfilled. The magnetization reversal in rotation field seems to be the best approach for the model.

In the present paper the results of galvanomagnetic effect study in thin permalloy films at uniaxial stress in a rotation magnetic field are reported.

2. Theoretical

Assume the current I to flow along the x-axis in a single domain thin ferromagnetic film lying in the xy-plane. An electric field then arises with components ε_x and ε_y in the direction of x and y, respectively [10–12]. The voltage U_y belonging to the field component ε_y is given by the expression

$$U_y = \frac{\Delta\varrho I}{2d} \sin 2\phi, \tag{1}$$

* Address: Instytut Fizyki Molekularnej PAN, Smoluchowskiego 17/19, 60–179 Poznań, Poland.

where $\Delta\varrho = \varrho_{\parallel} - \varrho_{\perp}$ is the difference in resistivities of the film when the magnetization vector $\vec{M}_s$ is directed parallel and perpendicularly to the current I, respectively; ϕ is the angle between $\vec{M}_s$ and I; and d is the film thickness.

In order to simplify the equations, U_y was normalized as follows

$$u_y = U_y/U_{y(\max)} = \sin 2\phi, \tag{2}$$

where $U_{y(\max)}$ is the maximal galvanomagnetic voltage, occurring at $\phi = 45°$.

Let us assume the film to present uniaxial magnetic anisotropy with the easy axis L_{K_u} directed at the angle γ to x. We also assume externally introduced uniaxial stress σ to induce in the film plane an anisotropy with the easy axis L_{K_σ} at the angle θ to L_{K_u} (Fig. 1).

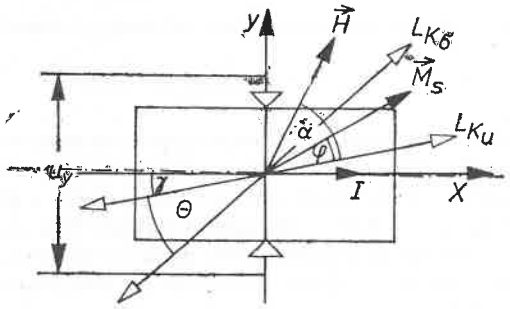

Fig. 1. Diagram of thin film: L_{K_u} — easy axis of magnetic uniaxial anisotropy, L_{K_σ} — easy axis of stress induced anisotropy, H — magnetic field, $\vec{M}_s$ — spontaneous magnetization vector

Now, if the film is additionally affected by an external magnetic field H at an angle α to the easy axis L_{K_u}, the free energy density related with the position of the magnetization vector can be written as follows

$$E(\varphi) = -M_s H \cos(\alpha - \varphi) + K_u \sin^2 \varphi + K_\sigma \sin^2(\varphi - \theta), \tag{3}$$

where K_u is the uniaxial anisotropy constant; $K_\sigma = \frac{3}{2}\lambda_s\sigma$ — the anisotropy constant, induced by stress σ in a material with the isotropic magnetostriction constant λ_s; and φ — the angle between $\vec{M}_s$ and the easy axis L_{K_u}. At equilibrium state, $\partial E(\varphi)/\partial\varphi = 0$ and $\partial^2 E(\varphi)/\partial\varphi^2 > 0$, Eq. (3) yields

$$-M_s H \sin(\alpha - \varphi) + K_u \sin 2\varphi + K_\sigma \sin 2(\varphi - \theta) = 0. \tag{4}$$

On substituting $\phi = \gamma + \varphi$ into Eq. (2), one gets

$$u_y = \sin 2(\gamma + \varphi). \tag{5}$$

From Eqs (4) and (5), we obtain the general relation between the galvanomagnetic voltage u_y and the external field H and its direction α, the anisotropy field $H_K = 2K_u/M_s$ and anisotropy field induced by stress $H_\sigma = 2K_\sigma/M_s$ and the directions of their axes γ and θ, in the following form

$$H_K(u_y \cos 2\gamma \mp \sqrt{1-u_y^2}\sin 2\gamma) + H_\sigma[u_y \cos 2(\theta+\gamma) \mp \sqrt{1-u_y^2}\sin 2(\theta+\gamma)]$$
$$-H\sqrt{2}\left[\sqrt{1 \pm \sqrt{1-u_y^2}}\sin(\alpha+\gamma) - \sqrt{1 \mp \sqrt{1-u_y^2}}\cos(\alpha+\gamma)\right] = 0 \tag{6}$$

or equivalently,

$$H\{\sin\alpha[\cos\gamma(\sqrt{1+u_y}+\sqrt{1-u_y})+\sin\gamma(\sqrt{1+u_y}-\sqrt{1-u_y})]$$
$$-\cos\alpha\cos\gamma(\sqrt{1+u_y}-\sqrt{1-u_y})-\sin\gamma(\sqrt{1+u_y}+\sqrt{1-u_y})]\}$$
$$-H_K(u_y\cos 2\gamma-\sqrt{1-u_y^2}\sin 2\gamma$$
$$-H_\sigma[\cos 2\theta(u_y\cos 2\gamma-\sqrt{1-u_y^2}\sin 2\gamma)-\sin 2\theta(\sqrt{1-u_y^2}\cos 2\gamma+u_y\sin 2\gamma)]=0. \quad (6a)$$

In these equations, for values in the first quadrant, the upper signs correspond to $\vec{M}_s$ lying in the interval $0^0 \leqslant \varphi \leqslant 45°$ and the lower signs to $45° \leqslant \varphi \leqslant 90°$. In the remaining quadrants, the signs have to be chosen appropriately.

As a simplification, we assume that in the stress-free film the direction of the easy axis L_{K_u} coincides with that of the current $I(\gamma = 0)$. We shall now consider the case when the stress induces the anisotropy axis L_{K_u} parallel or perpendicularly to the axis L_{K_u}. Now $\theta = 0°$ or $\theta = 90°$, and Eq. (3) becomes

$$E(\varphi) = -M_sH\cos(\alpha-\varphi)+(K_u+K_\sigma)\sin^2\varphi. \quad (7)$$

It is assumed that $K_\sigma > 0$ if $\theta = 0°$ and $K_\sigma < 0$ if $\theta = 90°$.

On denoting the constant of effective anisotropy by $K'_{\text{eff}} = K_u \pm K_\sigma$ and subsequently the field of this anisotropy by $H'_{K_{\text{eff}}} = 2K'_{\text{eff}}/M_s$, and on normalizing the applied magnetic field as follows: $h^* = H/H'_{K_{\text{eff}}}$, from Eq. (6) we obtain [8]

$$h^* = u_y/\sqrt{2}\,(\sqrt{1\pm\sqrt{1-u_y^2}}\sin\alpha-\sqrt{1\pm\sqrt{1-u_y^2}}\cos\alpha), \quad (8)$$

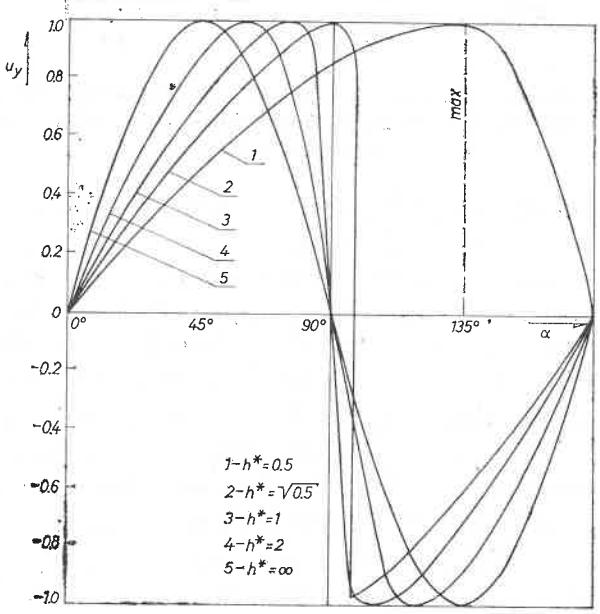

Fig. 2. Curves of galvanomagnetic voltage u_y vs the angle α of the applied magnetic field, normalized to the effective anisotropy field, $h^* = H/H'_{K_{\text{eff}}}$

or from Eq. (6a),

$$h^* = u_y/[(\sqrt{1+u_y}+\sqrt{1-u_y})\sin\alpha-(\sqrt{1+u_y}-\sqrt{1-u_y})\cos\alpha. \tag{8a}$$

The galvanomagnetic voltage as a function of the direction of applied magnetic field (expressed by h^*), is shown in Fig. 2.

The value of h^* increases with the increase of H and decreases with increasing H_σ. At $H_\sigma < 0$ and $|H_\sigma| > H_K$ simultaneously, the effective anisotropy field $H'_{\text{eff}} = H_K - H_\sigma$ becomes negative, corresponding to a rotation of the easy axis of this anisotropy by $\pi/2$. It is apparent that $H_\sigma > 0$ for $\lambda_s > 0$ and $\sigma > 0$ as well as for $\lambda_s < 0$ and $\sigma < 0$, tensile stress being counted as positive.

The position of the extrema of the rotation curve (Fig. 2) is a function of the field h^*. Let us consider solely the maxima closest to the axis of ordinates, for which $u_{y(\max)} = 1$.

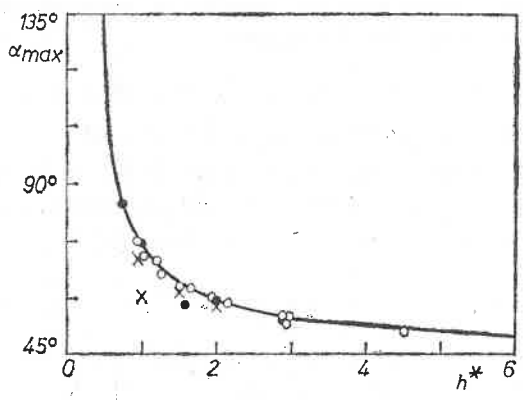

Fig. 3. The angle $\alpha_{\max}$ at which the maximum of the curves occurs, vs the normalized field h^*. The continuous line is the theoretical curve. The points are experimental results: full circles — $H_\sigma = 0$, open circles — $H_\sigma > 0$, crosses — $H_\sigma < 0$

As h^* decreases from infinity to 1/2, the angle $\alpha_{\max}$ defining the position of the maximum of the curve increases from 45° to 135° (Fig. 3).

The theoretical rotation curves derived from Eqs (6) or (6a), as compared with experimental ones will be discussed in the following part of this paper. Fig. 4 shows curves of $u_y = f(\alpha)_{h_\sigma,h}$ for the case when $\theta = 0°$. The normalized stress-induced anisotropy field, $h_\sigma = H_\sigma/H_K$, is assumed as parameter for various curves whereas Figs 4a, b, c and d are plotted for the normalized applied field $h = H/H_K$, for the values 0.5, $\sqrt{0.5}$, 1.0 and 2.0, respectively. One readily notes that for fields h corresponding to values $h^* < 1/2$ the curve shapes exhibit a period of 2π, whereas on exceeding this value the peroid is π. The position of the maxima of these curves given by the angle $\alpha_{\max}$, for which $u_y = 1$, is shown as a function of h_σ for $h = 0.5$, $\sqrt{0.5}$, 1.0 and 2.0 in Fig. 5. At $h_\sigma > -1$ the angle $\alpha_{\max}$ is seen to grow from 45° to 135°. The angle $\alpha_{\max}$ takes values larger than 135° when $u_{y(\max)}$ no longer attains the value 1, and the dependence of $\alpha_{\max}$ on h_σ ceases to be meaningful for the above interpretation. In the range of $h_\sigma < -1$, as the easy axis

performs a jump of $\pi/2$, the position of the maximum for the curve shifts continuously into the interval of angles smaller than 45° (Fig. 4b — $h_\sigma = -(1-\sqrt{2}/2)$ and $h_\sigma = -(1+\sqrt{2}/2)$.

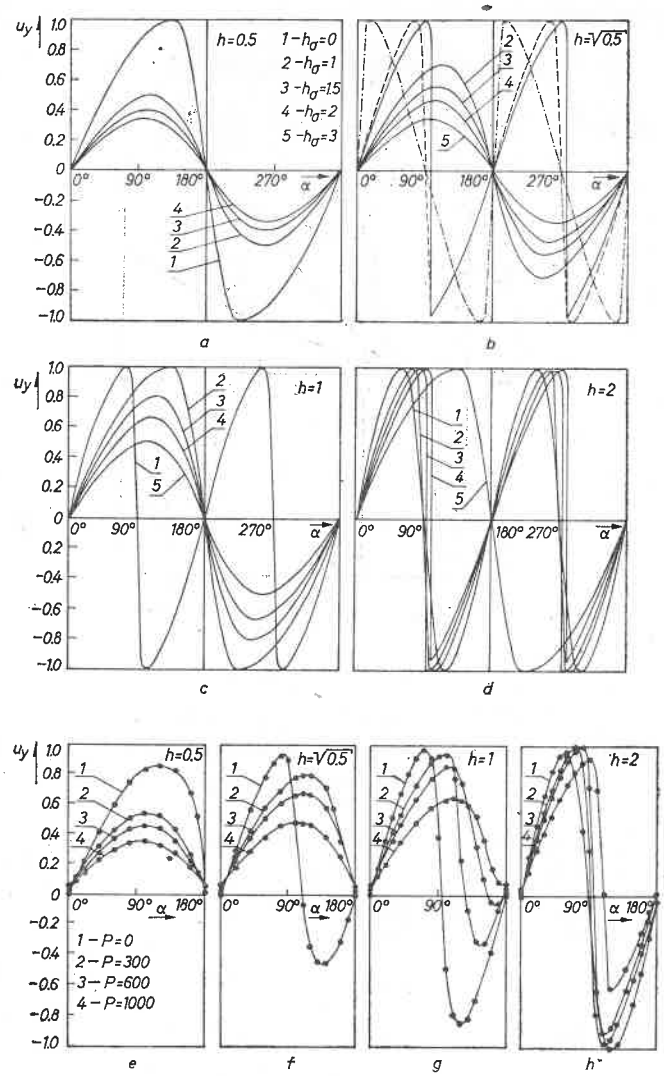

Fig. 4. Theoretical (a–d) and experimental (e–h) rotation curves of galvanomagnetic voltage, for $\theta = 0°$. In Fig. 4b curves for $h_\sigma = -(1-\sqrt{2}/2)$ (dashed line) and $h_\sigma = -(1+\sqrt{2}/2)$ (dash-dotted line), are plotted

In the case discussed above, the introduction of uniaxial stress affects in general only the value of the effective anisotropy but leaves its direction unaffected. If, however, $\theta \neq 0°$ and $\theta \neq 90°$ a change in stress entails a change in direction of the effective anisotropy

also. In this case, for $\gamma = 0°$, Eq. (6) takes the form

$$u_y + h_\sigma(u_y \cos 2\theta \pm \sqrt{1-u_y^2} \sin 2\theta) - h\sqrt{2}\,(\sqrt{1 \pm \sqrt{1-u_y^2}} \sin\alpha - \sqrt{1 \mp \sqrt{1-u_y^2}} \cos\alpha) = 0, \tag{9}$$

whereas Eq. (6a) becomes

$$u_y + h_\sigma(u_y \cos 2\theta \mp \sqrt{1-u_y^2} \sin 2\theta)$$
$$-h[(\sqrt{1+u_y} + \sqrt{1-u_y}) \sin\alpha - (\sqrt{1+u_y} - \sqrt{1-u_y}) \cos\alpha] = 0. \tag{9a}$$

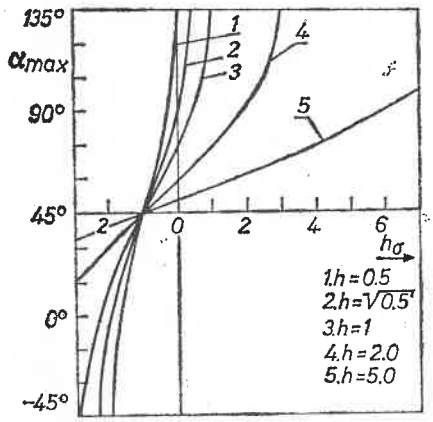

Fig. 5. Angle α_{max} vs h_σ, with h as parameter

These two equations are rather complicated and by no means easily accessible to interpretation. We consequently shall attempt to solve the problem otherwise [14].

Let us denote the angle between the axis of effective anisotropy and the axis L_{K_u} by β. The equation of magnetic energy density can now be written as follows

$$E(\varphi) = -M_s H \cos(\alpha - \varphi) + K_{eff} \sin^2(\varphi - \beta) + K_0, \tag{10}$$

where K_{eff} is the effective anisotropy constant, and K_0 — a constant. Equating the anisotropy energy of Eqs (3) and (10) we obtain

$$E_a(\varphi) = K_{eff} \sin^2(\varphi - \beta) + K_0 = K_u \sin^2\varphi + K_\sigma \sin^2(\varphi - \theta). \tag{11}$$

Minimization of the right hand term of (11) with regard to the angle φ yields [9]

$$\operatorname{tg} 2\beta = \frac{K_\sigma \sin 2\theta}{K_u + K_\sigma \cos 2\theta} = \frac{h_\sigma \sin 2\theta}{1 + h_\sigma \cos 2\theta}. \tag{12}$$

This formula expresses the rotation of the easy axis in the film under the influence of applied stress. On the other hand, we have by Eq. (11)

$$K_{eff} = \frac{K_u + K_\sigma \cos 2\theta}{\cos 2\beta} = \sqrt{K_u^2 + K_\sigma^2 + 2K_u K_\sigma \cos 2\theta},$$

or

$$h_{\text{eff}} = \sqrt{1+h_\sigma^2+2h_\sigma \cos 2\theta}\,, \tag{13}$$

and

$$K_0 = K_\sigma \sin^2\theta - K_{\text{eff}} \sin^2\beta = \tfrac{1}{2}(K_u + K_\sigma - K_{\text{eff}}). \tag{14}$$

Now since K_0 does not depend on φ it can be neglected in Eq. (10) and angle φ hence determined substituted into Eq. (5). This procedure, however, would yield an equation just as complicated as (10) and (10a). For $\gamma = 0$, it is of the form

$$h_{\text{eff}}(u_y \cos 2\beta \pm \sqrt{1-u_y^2} \sin 2\beta)$$

$$-h[(\sqrt{1+u_y}+\sqrt{1-u_y}) \sin\alpha - (\sqrt{1+u_y}-\sqrt{1-u_y}) \cos\alpha] = 0. \tag{15}$$

The difficulties in the interpretation of this equation can be by passed by having recourse to the graphical method of determining the angle φ by means of the asteroid. The necessery values of β and h_{eff} are to be determined from Eqs (12) and (13).

Theoretical curves of the galvanomagnetic voltage u_y vs the direction of the applied magnetic field are shown in Figs 6, 7, 8 and 9 for various values of the field and stress. Each of the figures contains four theoretical graphs (a, b, c, d) and four experimental ones (e, f, g, h), plotted for different values of the normalized external field h and each of the graphs contains a family of curves with the stress as parameter. The stress, for the theoretical curves, is expressed in terms of the anisotropy field induced by the stress, h_σ, whereas in the case of the experimental ones it is expressed by the bending load P on the sample.

Fig. 6 shows rotation characteristics of the voltage u_y for stress applied at an angle of $\theta = 30°$. In this case, rotation of the easy axis under the stress is rather small because it cannot exceed the angle θ i.e. $0° \leqslant \beta \leqslant 30°$. At a constant value of the field h, an increase in stress causes however a change in position of the magnetization vector not only by way of an increase in β but also by way of an increase in value of the effective anisotropy field h_{eff}.

It is shown in [13] how, in the case when two uniaxial anisotropies exist in the film at some angle to each other, the effective anisotropy changes in value and position as one of the two anisotropies undergoes a variation in value. Hence, in the case of uniaxial stress also, the contribution from rotation of the axis and the value of the effective anisotropy is different for the individual curves.

In Figs 7, 8 and 9 the angle θ amounts to 45°, 60° and 80°, respectively (for the theoretical curves). The contribution of rotation of the easy axis to the change in position of the magnetization vector is thus increasingly larger in this case. But the contribution of the change in value of effective anisotropy is the least for $\theta = 60°$ as h_σ grows from 0 to a value not much larger than unity. $H_{K_{\text{eff}}}$ then assumes a value close to H_K although (as is the case for all angles $\theta > 45°$) $K_{K_{\text{eff}}}$ in this case decreases with the increasing H from a value equal to H_K down to some minimal value $H_{K_{\text{eff(min)}}}$ then starts to increase in this particular case — to $H_K\sqrt{3}/2$.

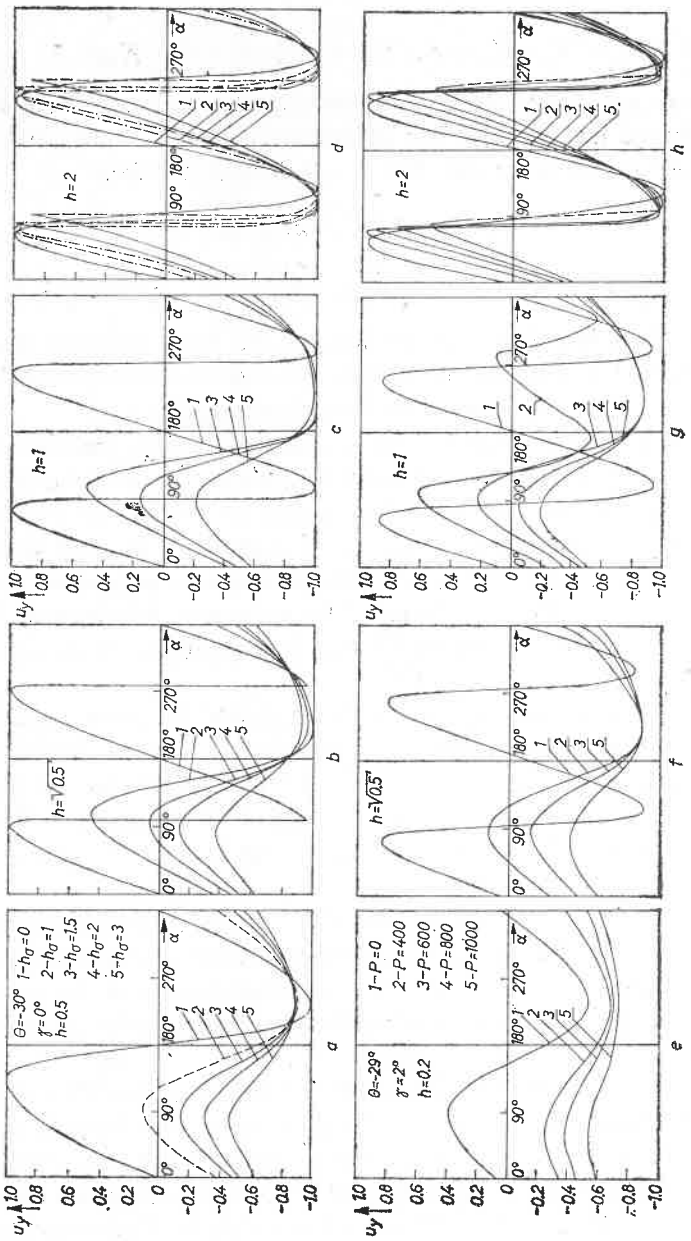

Fig. 6. Theoretical (a–d) and experimental (e–h) rotation curves, for $\theta = 30°$

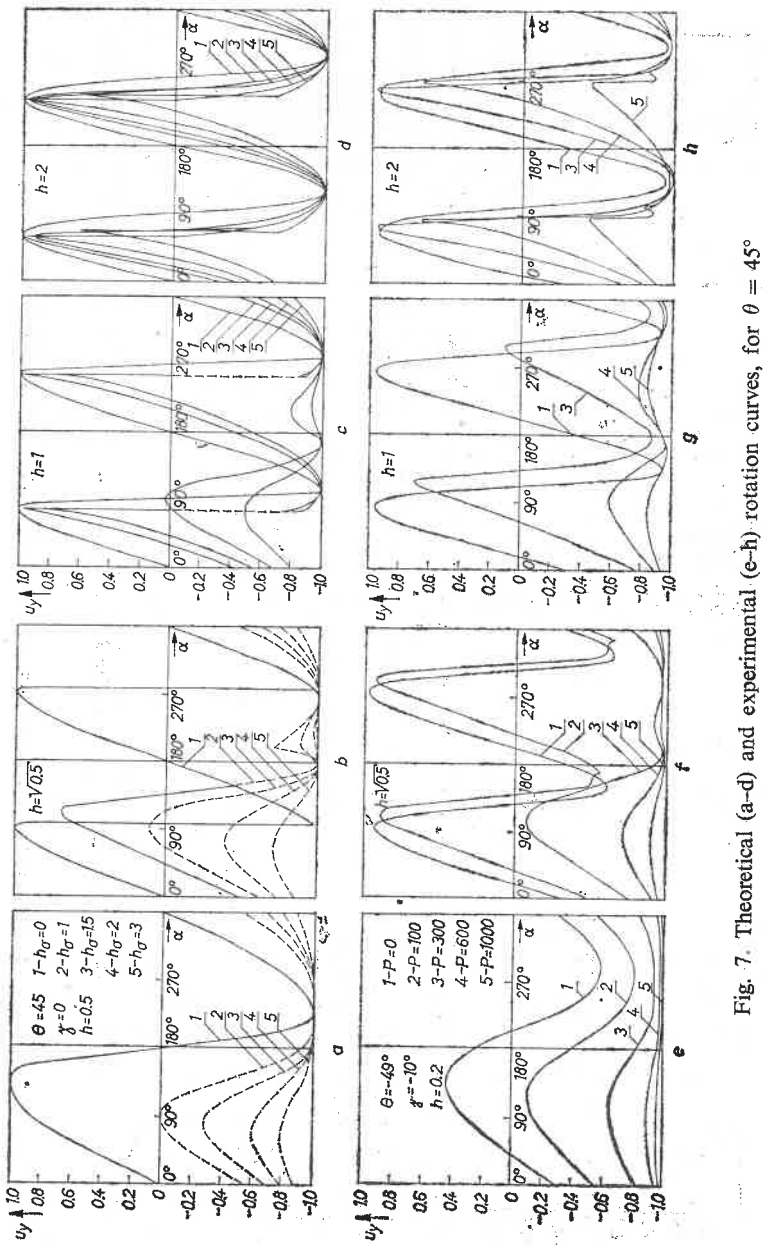

Fig. 7. Theoretical (a–d) and experimental (e–h) rotation curves, for $\theta = 45°$

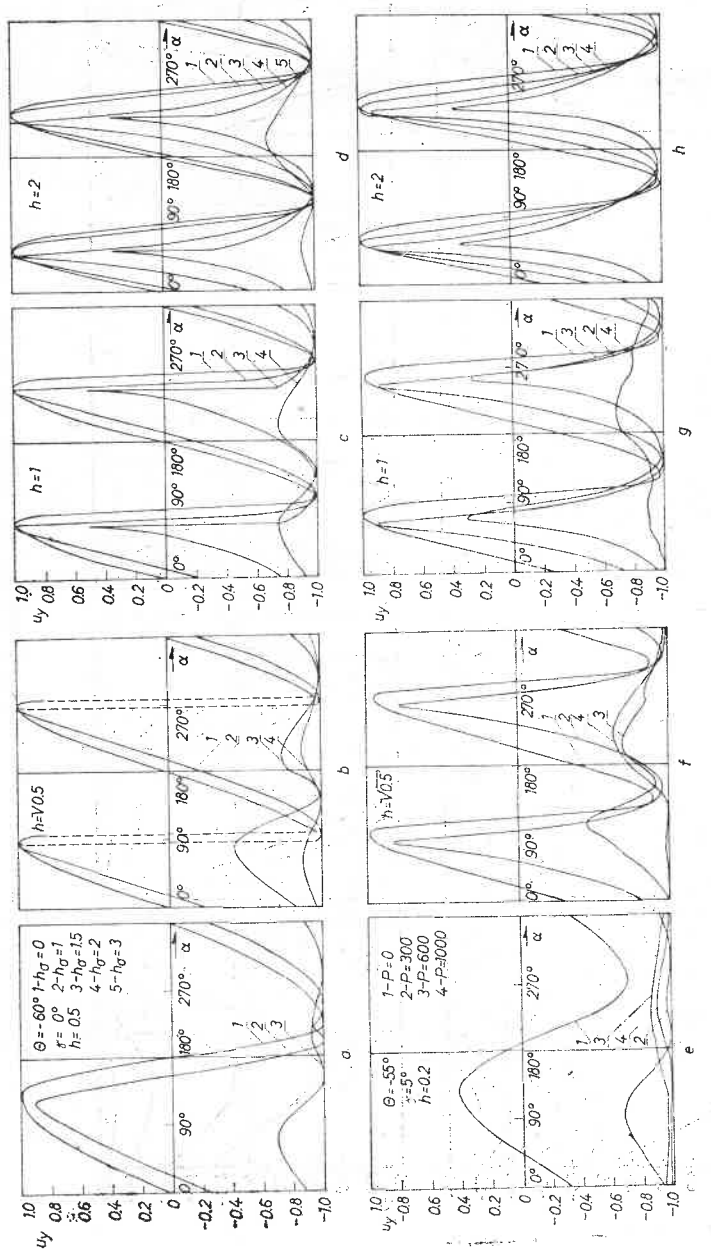

Fig. 8. Theoretical (a–d) and experimental (e–h) rotation curves, for $\theta = 60°$

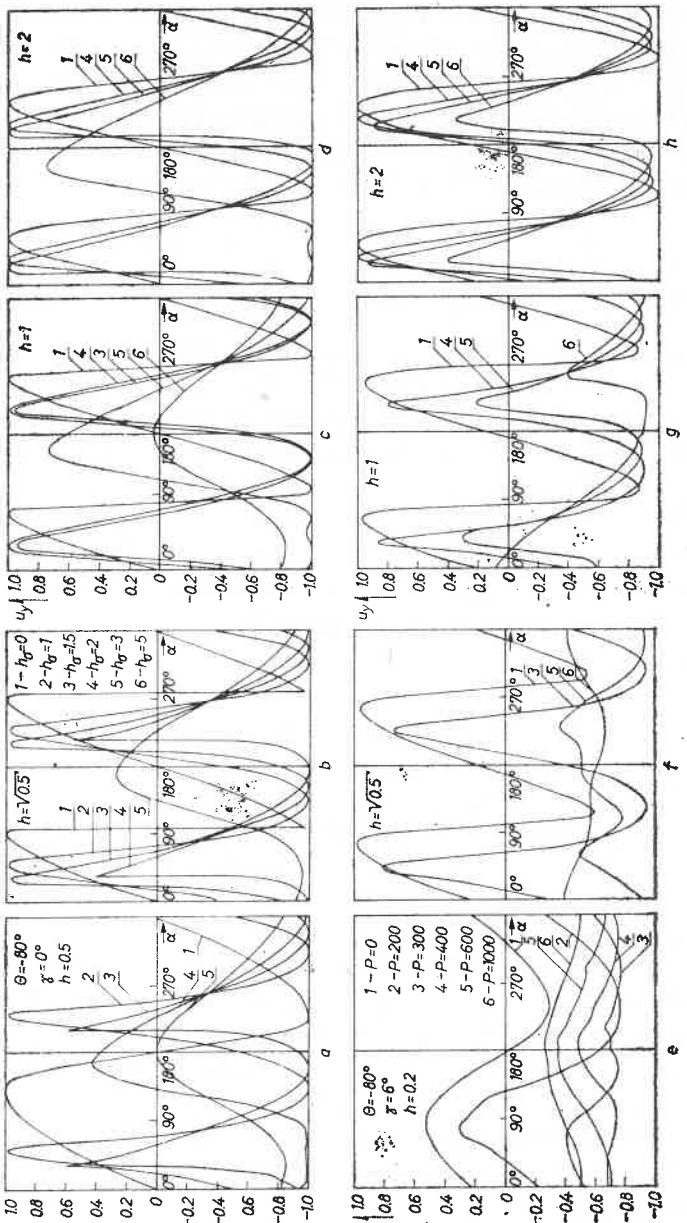

Fig. 9. Theoretical (a–d) and experimental (e–h) rotation curves, for $\theta = 80°$

The effect resulting from the rotation of the effective anisotropy axis appears chiefly as a shift in galvanomagnetic voltage in the point $\alpha = 0°$, for the various graphs. Changes in value of the effective anisotropy become apparent essentially by a change in amplitude of the galvanomagnetic voltage, when $H/H_{K_{eff}} < 0.5$. The position of the extrema of the curves obviously depends both on rotation of the axis $L_{K_{eff}}$ and on the value of $H_{K_{eff}}$.

Contrary to the case $\theta = 0°$ (Fig. 4), when the rotation curves are symmetric with respect to the point $\alpha = 180°$, $u_y = 0$, no such symmetry is exhibited by the curves for $\theta \neq 0°$ and $\theta \neq 90°$. This is due to the simultaneous action on the magnetization vector $\vec{M}_s$ of the rotation of the easy axis and a change in value of the effective anisotropy, in the latter case.

3. Experimental procedure

In order to check to what extent the results of the preceding considerations based on the model of the simple coherent rotation of $\vec{M}_s$ [14] are in accordance with experiment, we carried out an experimental study on samples with parameters close to those assumed above. The samples were films of the composition 85% Ni, 11% Fe and 4% Mo deposited by evaporation in vacuum of about 2×10^{-6} Torr onto optical flat glass substrates of the size $10 \times 20 \times 1$ mm for the case when $\theta = 0°$ and $\theta = 90°$, and $15 \times 20 \times 1$ mm when $\theta \neq 0°$ and $\theta \neq 90°$. The films in the shape of 4×6 mm rectangles were equipped with evaporated silver electrodes. During the process of evaporation, the substrates were placed in a magnetic field of about 100 Oe directed parallel to the plane of the substrate, and the latter was heated to about 250°C.

The substrate holder permitted the deposition by evaporation of films of arbitrary geometrical orientation with respect to the edge of the substrate and having an arbitrarily directed anisotropy axis.

The film thickness was determined by the method of multibeam interference. The films were about 400 to 1400 Å thick. Preliminary measurements revealed the effect measured not to be dependent on the thickness of the film, throughout this interval.

Galvanomagnetic rotation curves were taken with a device consisting of a rotation support with angular scale, and Helmholtz coils. The support was equipped with a potentiometer, which gives a signal proportional to the angle of rotation with respect to the coils. The magnetic field could be varied continuously from $-10H_K$ to $+10H_K$ and was thus sufficiently strong to saturate the sample completely.

Uniaxial stress was introduced into the film by bending. The sample was placed on two prisms, 18 mm distant from each other, and was loaded with weights by means of a third prism, which exerted pressure on the sample at its centre. Using this device, in the range from $P = 0$ to 1 kg (which corresponds to a deflection of about 5 μm), the most reliable results were obtained.

The magnetic measurements started with the determination of coercive force and anisotropy field of the film from its hysteresis loop. Next, the sample was placed in the device for galvanomagnetic measurements, and, at zero load, the direction of the easy axis was determined. Setting the angular scale in this direction, rotation curves were

taken in a constant magnetic field $h = H/H_K$ increasing the load P gradually. Curves of $U_y = f(\alpha)_{P,h,\theta}$ were plotted by an $X-Y$ recorder (except the curves for $\theta = 0°$ and $\theta = 90°$, Figs 4e–h, which were taken point by point). Previous to taking each of the curves, the sample was magnetized to saturation in the easy axis direction in order to maintain its initially determined magnetic state.

The experimental curves obtained with the recording device were normalized with respect to $U_{y(\max)}$ as obtained in an applied field of $H = 10\,H_K$. This made comparison of the results easier.

4. Analysis of the results, and conclusions

In Fig. 4, experimental galvanomagnetic rotation curves are compared with the theoretical ones, for $\theta = 0°$. If one considers that the load P applied did not in general correspond to the theoretical values of h_a, two conclusions emerge immediately: (*i*) the shift in extrema of the curves obeys the theory, and (*ii*) the experimental values of $U_{y(\max)}$ are less than unity for nearly all values of h. The first conclusion is confirmed by the experimental points plotted in Fig. 3. The lowered values of $U_{y(\max)}$ clearly point to the presence of angular dispersion of anisotropy in the films [15, 16]. As the external field H

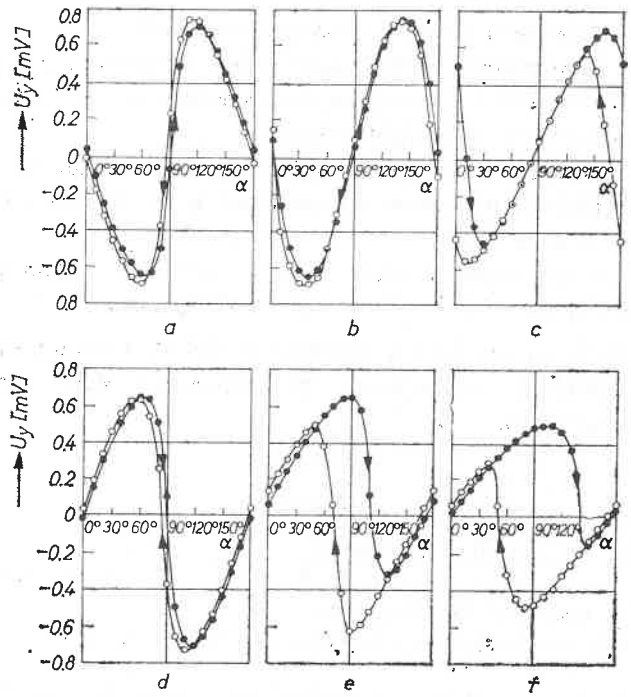

Fig. 10. Experimental rotation curves at rising and decreasing α: a, b, c — for positive stresses ($\theta = 0°$) $P = 0$, 300 and 600 g, respectively, and d, e, f — for negative stresses ($\theta = 90°$) with the same values. The negative stress was obtained by turning up the sample, hence the corresponding curves are inversed

and the effective anisotropy $H'_{K_{eff}}$ grow, the angular dispersion of anisotropy decreases and $U_{y(max)}$ increases in agreement with theoretical predictions.

In Figs 6–9, the experimental curves are compared with the theoretical ones for the angles $\theta = 30°, 45°, 60°$ and $80°$. One notes here a strong influence of anisotropy dispersion on the experimental curves, and this influence increases as θ grows. Obviously, a rotation of the axis of effective anisotropy will entail an increase in angular dispersion. This must be the more apparent the larger is the rotation angle β of the axis and the smaller is the applied magnetic field strength. The effect is well visible in Figs 6–9. At $\theta = 30°$ the discrepancy between the experimental and theoretical curves is insifgnificant but grows at $\theta = 45°$ and $60°$ to became very large at $\theta = 80°$.

The influence of anizotropy dispersion on the rotational magnetization reversal of a strained film could be more precisely estimated on the basis of rotational hysteresis diagram. Fig. 10 shows galvanomagnetic rotation curves determined for the increasing and decreasing α angle, ranging from 0° to 180° a, b and c curves refer to positive stresses ($\theta = 0°$): $P = 0$, 300 and 600 g, respectively; d, e, f curves refer to negative stresses ($\theta = 90°$). The rotational hysteresis increases evidently with the increase of stress, but the retrace curve is not in line with the original one even in sections with rotation reversal $\vec{M}_s$. The same effect is sharper for angles $\theta \neq 0°$ and $\theta \neq 90°$. It makes impossible to determine the rotational hysteresis dependence on the sample stress and thus on anizotropy dispersion increase.

The reported studies lead to the following conclusions:

(1) relatively good compatibility of the shape of experimental and theoretical curves in the majority of cases testifies to the rotation of the average easy axis of effective anisotropy to be in agreement with the theoretical model;

(2) discrepancies that occur under great loading of great θ angles can be explained by the anisotropy dispersion increase what is manifested by the decrease of maximum value of galvanomagnetic voltage U_{ymax};

(3) blocking effect of the ripple structure in films with such a great dispersion results in certain hysteresis in the range of reversible switching also.

The author wishes to express his gratitude to Dr. R. Gontarz and Z. Sczaniecki, M.Sc., for their valuable discussion and to M. Witkowska, M.Sc., for her help in the course of the measurements.

REFERENCES

[1] T. S. Crowther, *J. Appl. Phys.* **34**, 580 (1963).
[2] E. L. Mitchel, G. I. Lykken, G. D. Babcock, *J. Appl. Phys.* **34**, 715 (1963).
[3] R. L. Coren, *J. Appl. Phys.* **33**, 1168 (1962).
[4] V. A. Buravikhin, V. G. Kazakov, V. S. Khristosenko, P. J. Krukover, *Phys. Status Solidi* **16**, 651 (1966).
[5] T. Fujii, T. Tanaka, S. Uchiyama, Y. Sakaki, *Jap. J. Appl. Phys.* **10**, 1372 (1971).
[6] V. A. Dzhidarian, *Apparatura i metody issledovaniya tonkikh magnitnykh plenok*, Krasnoyarsk 1968, p. 110.
[7] C. Vautier, *J. Phys.* (France) **29**, 807 (1968).

[8] H. Ratajczak, R. Gontarz, W. Kwiatkowski, Z. Sczaniecki, M. Witkowska, *Czech. J. Phys.* **B21**, 503 (1971).
[9] H. Ratajczak, R. Gontarz, Z. Sczaniecki, M. Witkowska, *Proc. VI Intern. Coll. Magn. Thin Films*, Minsk 1973, 6.5; *Trudy mezhdunarod. koll. magn. plenkam*, Minsk 1973, Izdat. Vys. Shkola, Minsk 1974, p. 98.
[10] J. P. Jan, *Solid State Phys.* **5**, 1 (1957).
[11] Vu Din Ky, E. F. Kuritsyna, *Dokl. Akad. Nauk SSSR* **160**, 77 (1965).
[12] Z. Sczaniecki, R. Gontarz, W. Kwiatkowski, H. Ratajczak, *Phys. Status Solidi* (a) **7**, 597 (1971).
[13] Z. Sczaniecki, F. Stobiecki, R. Gontarz, H. Ratajczak, *Phys. Status Solidi* (a) **18**, 107 (1973)
[14] E. C. Stoner, E. P. Wohlfarth, *Philos. Trans.* (GB) **A240**, 599 (1948).
[15] T. Stobiecki, A. Paja, *Acta Phys. Pol.* **A41**, 343 (1972).
[16] T. Stobiecki, J. Spałek, H. Jankowski, *Acta Phys. Pol.* **A41**, 657 (1972).